Visible light-photosensitized oxidation of organic pollutants using amorphous peroxo-titania

Jiwon Seo[a], Hongshin Lee[a], Hye-Jin Lee[a], Min Sik Kim[a], Seok Won Hong[b], Jaesang Lee[c], Kangwoo Cho[d], Wonyong Choi[d], Changha Lee[a,*]

[a] School of Urban and Environmental Engineering, KIST-UNIST Ulsan Center for Convergent Materials (KUUC), Ulsan National Institute of Science and Technology (UNIST), Ulsan 44919, Republic of Korea
[b] Center for Water Resource Cycle Research, KIST School, University of Science and Technology (UST), Korea Institute of Science and Technology (KIST), Seoul 02792, Republic of Korea
[c] Department of Civil, Environmental, and Architectural Engineering, Korea University, Seoul 02841, Republic of Korea
[d] School of Environmental Science and Engineering, Pohang University of Science and Technology (POSTECH), Pohang 37673, Republic of Korea

ARTICLE INFO

ABSTRACT

Amorphous peroxo-titania (denoted as Am-peroxo-TiO$_2$), synthesized in this study by a facile method, demonstrated photochemical activity for the oxidation of organic pollutants under visible light illumination ($\lambda > 400$ nm). Am-peroxo-TiO$_2$ was synthesized by a one-step sol-gel method using titanium isopropoxide and hydrogen peroxide (H$_2$O$_2$) at room temperature and atmospheric pressure. The material produced was a yellow powdered precipitate; the measurement of diffuse reflectance confirmed light absorption of up to 600 nm. High-resolution transmission electron microscopy revealed that Am-peroxo-TiO$_2$ forms aggregates of small nanoparticles (ca < 10 nm). The surface peroxo-groups (Ti-OOH or Ti-OO-Ti) were characterized by Fourier-transform infrared spectroscopy and X-ray photoelectron spectroscopy. Visible light-illuminated Am-peroxo-TiO$_2$ completely degraded 10 μM 4-chlorophenol (4–CP) in 4 h. The photochemical activity of Am-peroxo-TiO$_2$ was selective to the target organic compound. Experiments using scavengers and probes of reactive oxidants revealed that reactive oxygen species such as hydroxyl and superoxide radicals are not responsible for the degradation of organic compounds. Liquid chromatography-mass spectrometry showed that 4–CP was oxidized to produce 4-chlorocatechol, hydroquinone, and benzoquinone as primary products. The results suggest that oxidation is initiated by electron abstraction or hydroxylation by the photogenerated reactive intermediates on the peroxo surface. Am-peroxo-TiO$_2$ was stable under both dark and illuminated conditions in the absence of organic compounds. Importantly, in the presence of organic compounds, the photochemical activity of Am-peroxo-TiO$_2$ gradually decreased. Further, platinization enhanced the photochemical activity as well as the stability of Am-peroxo-TiO$_2$.

1. Introduction

Titanium dioxide (titania, TiO$_2$) has been extensively studied as a photocatalyst for water purification owing to its low cost, (photo-) chemical stability, and high photooxidizing potential [1–4]. Light illumination on TiO$_2$ induces charge separation on surfaces to generate electron-hole pairs, which subsequently lead to redox reactions. Light-illuminated TiO$_2$ in aqueous suspension usually produces reactive oxygen species (ROS) such as hydroxyl and superoxide radicals (·OH and O$_2$·$^-$). ·OH and O$_2$·$^-$ are typically produced via hole-oxidation of water molecules and the electron-reduction of oxygen, respectively. These ROS and photogenerated holes can be used to oxidatively

degrade recalcitrant organic pollutants. However, the photochemical activity of TiO$_2$ is limited to the ultraviolet (UV) region of the light spectrum as evidenced by the wide band gap (ca 3.0 and 3.2 eV for rutile and anatase phases, respectively) [4,5]. To extend the range of wavelength for TiO$_2$, different approaches have been attempted, including metal and non–metal doping [6–8], dye photosensitization [9,10], and coupling with narrow band gap semiconductors [11,12].

Further, several studies have reported that the interaction of TiO$_2$ with hydrogen peroxide (H$_2$O$_2$) can generate visible light responsive photochemical activity [13–16]. The addition of H$_2$O$_2$ to the aqueous suspension of TiO$_2$ leads to the formation of peroxo-complexes on the TiO$_2$ surface [13,14,16]. It has been suggested that these peroxo-titania

complexes are photoexcited by visible light, which can lead to the transfer of electrons, permitting the conduction band of TiO_2 that subsequently reduces adsorbed H_2O_2 to ·OH [13]. TiO_2 with externally supplied H_2O_2 has been found to degrade salicylic acid [13] and methylene blue [16], and oxidize 1-decene to an epoxide [14] under visible light illumination.

Although TiO_2 as a photocatalyst has been actively studied, the synthesis of peroxo-titania complexes as a stable solid material has been seldom reported and discussed. There have been a few cases where H_2O_2 was used to synthesize oxygen-rich TiO_2, which exhibited visible light responsive activity, causing the degradation of methylene blue [17] and the reduction of carbon dioxide [18]. Of significance, these oxygen-rich TiO_2 products did not have any peroxo-complexes on the surface (in the synthetic process, peroxo-titania complexes are formed as intermediates, but they disappear during calcination). Therefore, the photochemical activity and mechanisms observed to date are entirely different from those of peroxo-titania discussed here. One study has reported the synthesis of peroxo-titania and its use for methanol oxidation under visible light illumination [15]. However, the aforementioned study strikingly differs from this study due to the following: i) the synthetic conditions were harsher and more complicated (e.g., the use of ammonia and commercial TiO_2 powder, autoclaving step for 12 h, etc.); ii) the photochemical activity and mechanism of the material were different from ours (refer to the results and discussion parts for details); and iii) no interpretations were offered for the oxidation pathways of the organic compounds (i.e., the oxidation pathways were not elucidated).

In this study, amorphous peroxo-titania (Am-peroxo-TiO_2) was synthesized by a simple method only using titanium(IV) precursor and H_2O_2 under mild conditions. The synthesized material was characterized by different surface analytical tools, and its photochemical activity to oxidize organic pollutants were examined under visible light illumination ($\lambda > 400$ nm). Lastly, to elucidate the mechanism through which the organic compound was oxidized, experiments using probes and scavengers of ROS were performed, where the oxidation products were analyzed using mass-spectroscopy.

2. Materials and methods

2.1. Reagents

All chemicals were reagent grade and used without further purification. Chemicals used in this study included: titanium(IV) isopropoxide (TIP), H_2O_2, sodium hydroxide, perchloric acid, phenol, 4–chlorophenol (4–CP), benzoic acid (BA), acetaminophen (AAP), carbamazepine (CBZ), methanol, *tert*–butanol, phosphoric acid, 1.10 phenanthroline, *para*–hydrobenzoic acid (*p*-HBA), coumarin, 7-hydroxycoumarin (7-HC), 2,3-bis(2-methyl-4-nitro-5-sulfophenyl)-2H-tetrazolium-5-carboxanilide (XTT), and 5,5-dimethyl-1-pyrroline N-oxide (DMPO) (all purchased from Sigma–Aldrich Co.). Other materials used were TiO_2 powder (P25, Degussa Co.) and acetonitrile (J.T. Baker Co.). All solutions were prepared in deionized (DI) water (18 MΩ cm Milli–Q water, Millipore Co.). Stock solutions of phenol (10 mM), 4–CP (10 mM), BA (10 mM), AAP (1 mM), CBZ (0.1 mM), coumarin (1 mM), and XTT (1 mM) were prepared and stored at 4 °C until use.

2.2. Synthesis

Am-peroxo-TiO_2 was synthesized by the sol–gel method. 2 mL TIP was mixed with 10 mL H_2O_2 solution (1 M), where the mixture was stirred for 1 h at room temperature (22 ± 2 °C). The resulting gel was collected by centrifugation at 3000g for 15 min, and subsequently washed three times with DI water. Next, the gel was dried at 50 °C for 4 h to obtain the powdered sample. For the control test, the TiO_2 powder was synthesized by the same method in the absence of H_2O_2; all steps were identical, but DI water was used in place of the 1 M H_2O_2 solution.

Platinized Am-peroxo-TiO_2 (Pt-Am-peroxo-TiO_2) was synthesized as follows. 1.25 mL TIP and 25 mL ethanol were added to a 250 mL acidic solution (pH 1.5 maintained with nitric acid), containing 1 M H_2O_2 and 0.08 mM chloroplatinic acid (H_2PtCl_6), and stirred overnight. The resulting gel was evaporated at 50 °C. The final powder product was washed with DI water and dried at 50 °C for 4 h.

2.3. Characterization

X–ray diffraction patterns of the synthesized materials were recorded using an X-ray diffractometer (D8 ADVANCE, Bruker AXS Inc.) with Cu–Kα radiation. Morphology and surface elemental distribution were analyzed with a high–resolution transmission electron microscope, coupled with an energy dispersive X-ray spectrometer (HRTEM/EDX) at 200 kV (JEM–2100F, Jeol Co.). X-ray photoelectron spectroscopy (XPS) with monochromatic Al–Kα radiation (K–alpha, Thermo Fisher Scientific Inc.) and Fourier transform infrared (FT–IR) spectroscopy (Nicolet 6700, Thermo Fisher Scientific Inc.) were used to examine the surface compositions and functional groups of the powdered products. A UV/vis/near IR spectrophotometer (Cary 5000, Agilent Co.) was used to obtain the diffuse reflectance spectra. Specific surface area (SSA) of the powder was determined by the 5 point Brunauer–Emmett–Teller (BET) method using N_2 physisorption measurements on an ASAP 2420 Accelerated Surface Area and Porosimetry system (Micromeritics Co.).

2.4. Photochemical experiments

All experiments were performed in a quartz batch reactor at room temperature (22 ± 2 °C). For most experiments, light illumination was performed using fluorescent lamps (six 4 W lamps; Shin–Kwang electronics Co.) with a 400 nm longpass filter in a dark chamber. For few of the experiments, illumination was performed by a 150 W xenon arc lamp (LS 150, Abet Technologies Inc.) equipped with an AM 1.5G filter and a 400 nm longpass filter; the light intensity with AM 1.5G filter was adjusted to one–sun condition (100 mW/cm^2). Light emission spectra of the fluorescent lamp and the xenon arc lamp were recorded by a spectroradiometer (SPR-4001, Luzchem Research Inc.) (Fig. S1 in the supplementary data).

The reaction solution (50 mL) was prepared by adding the powder (0.5 g/L) and the target organic compound (10 μM). Initial pH of the solution was adjusted at 5.0, and pH variations during the reaction were maintained at less than 0.2 units. Initiation of the reaction occurred upon light illumination. The incident photon, which flowed into the reaction solution were 6.43×10^{-6} Einstein/L s (fluorescent lamp) and 2.46×10^{-5} Einstein/L s (xenon arc lamp), were measured by chemical actinometry using the potassium Reinecke's salt (400 ∼ 650 nm) [19]. The abovementioned values were converted to 1.45 mW/cm^3 and 5.61 mW/cm^3, respectively, where the calculation was derived from the respective light emission profiles shown in Fig. S1. During the photochemical reaction, samples (1 mL) were withdrawn at predetermined time intervals, and immediately filtered using a 0.45 μm PTFE syringe filter (Advantech Co.). All experiments were performed in triplicates, at a minimum. Average values and standard deviations (error bars) have been presented.

2.5. Analytical methods

The concentrations of the organic compounds were measured by high performance liquid chromatography (HPLC, UltiMate™ 3000, Dionex Co.) with UV absorbance detection (at 277, 230, 227, 241, 285, 270, and 320 nm for phenol, 4–CP, BA, AAP, CBZ, *p*–HBA, and 7–HC, respectively). Separation was performed on a 150 mm × 4.6 mm, 5 μm C18 column (ZORBAX Eclipse XDB–C18, Agilent Co.). A mixture of phosphoric acid solution (0.1%v/v), acetonitrile, and methanol was used as the mobile phase at a flow rate of 1 mL/min. Chloride ion was

measured by ion chromatography (ICS 2100, Dionex Co.) equipped with a conductivity detector. Separation was performed on a Dionex IonPac As-16 column using 22 mM potassium hydroxide solution as the mobile phase at a flow rate of 1 mL/min. The concentration of total organic carbon (TOC) was determined by TOC analyser (TOC-V/CPH, Shimadzu Co.). The degradation products of 4-CP were analyzed by the rapid separation liquid chromatography (RSLC) (UltiMate 3000, Dionex Co.) system coupled with a quadrupole-Orbitrap mass spectrometer (Q Exactive™, Thermo Fisher Scientific Inc.) (LC/MS). Detailed conditions for the LC/MS analysis are described in the supplementary data (Text S1). Photocurrents were measured of the aqueous suspensions of Am-peroxo-TiO_2 and Pt-Am-peroxo-TiO_2 containing 1 mM Fe(III) as an electron shuttle and 0.1 M $NaClO_4$ as an electrolyte under visible light conditions (xenon arc lamp) [20]. A three-electrode cell with platinum plates (2.5 cm x 1.5 cm), serving as working and counter electrodes, and a saturated calomel electrode (SCE) as a reference electrode, were used. Currents were recorded using a potentiostat (VSP, Bio-Logic Science Instruments) with the chronoamperometry mode on a working electrode biased at + 0.7 V (vs. SCE). An electron paramagnetic resonance (EPR) spectroscopy (JES-X310, Jeol Co.), using 10 mM DMPO as a spin-trapping agent, was used to detect ROS. Samples were collected from the photochemical reactor, and transferred into a quartz flat cell for the EPR analysis. EPR signals of the DMPO-radical adducts were scanned under the following conditions: microwave frequency at 9.42 GHz, microwave power at 1.00 mW, modulation frequency at 100 kHz, and modulation amplitude at 2.0 G.

3. Results

3.1. Synthesis and characterization of Am-H_2O_2-TiO_2

In preliminary experiments, different varieties of Am-peroxo-TiO_2 were synthesized using varying concentrations of H_2O_2 (for the sol-gel process) and the drying temperature, and then their photochemical activity to degrade 4-CP were examined under visible-light illumination (Fig. S2 in the supplementary data). The yellow color of the powdered substance intensified with increasing concentrations of the H_2O_2 utilized in the synthetic process (Fig. S2a). Importantly, the degradation rate of 4-CP was optimized when 1 M H_2O_2 was used to synthesize the powdered precipitate (Figs. S2b and c). Interestingly, the yellow color of the material faded with increasing temperatures (Fig. S2d) during the drying process, and correspondingly the degradation rate of 4-CP drastically decreased when dried at temperatures higher than 100 °C (Figs. S2e and f). Based on these results, the synthetic conditions of Am-peroxo-TiO_2 for photochemical experiments were selected, where 1 M H_2O_2 (the concentration of H_2O_2 used in the sol-gel process) and 50 °C (the drying temperature) were used for the present study.

The Am-peroxo-TiO_2 material product was a yellow powdered precipitate, with a diffuse reflectance spectrum of visible light absorption of up to 600 nm (Fig. 1a). XRD patterns of Am-peroxo-TiO_2 recorded mostly amorphous phases with poor crystallinity; and Am-peroxo-TiO_2 exhibited very weak and broad anatase peaks (Fig. 1b). Calcination of Am-peroxo-TiO_2 at elevated temperatures can enhance the anatase phase (Fig. S3a) with crystal particle growth through the sintering process (Fig. S3b). However, as shown in Fig. S2, heat treatment appears to destroy any surface peroxo complexes of Am-peroxo-TiO_2, thereby eliminating its photochemical activity. HRTEM images indicated that Am-peroxo-TiO_2 forms aggregates of small nanoparticles (ca < 10 nm) (Fig. 1c). The specific surface area of Am-peroxo-TiO_2 was determined to be 267.89 m^2/g, which is approximately 5-fold greater than that of commercial TiO_2 (Degussa P25, average particle size is 25 nm; specific surface area is 52.68 m^2/g). Additionally, HRTEM-EDX analysis indicates that Am-peroxo-TiO_2 has a high atomic oxygen to titanium ratio (O:Ti = 46.1:53.9), possibly due to the presence of its surface peroxo groups (Fig. 1d); the O:Ti atomic ratio of P25 has been measured to be at 33.1:66.9.

The O 1 s XPS spectrum of Am-peroxo-TiO_2 revealed three bands (Fig. 2a). The bands at 529.8 and 531.8 eV represent the lattice oxygen (Ti^{4+}–O) and the hydroxide oxygen (Ti^{4+}–OH), respectively [14,21]. The band at 533 eV correlates to the peroxo complexes, Ti^{4+}–OOH [21]. However, the XPS spectrum of P25 did not reveal a band corresponding to the peroxo complex, and only displayed a small hydroxide band relative to that of Am-peroxo-TiO_2 (Fig. S4 in the supplementary data). In addition, the FT-IR spectrum registered absorbance bands reflecting the surface peroxo groups in the range of 950–700 cm^{-1}, resulting from the stretching vibrations of the −O−O− bonds [14,22]. The Ti-peroxo groups are known to have two different species (i.e., Ti–η^2–peroxide (932–800 cm^{-1}) and Ti–μ–peroxide (770–700 cm^{-1})) [14,22]. The FT–IR spectrum of Am-peroxo-TiO_2 displayed an absorption band centered at 900 cm^{-1} that was attributable to Ti–η^2–peroxide (Fig. 2b).

3.2. Photochemical degradation of organic compounds

Degradation of 4-CP by Am-peroxo-TiO_2 and the respective control materials (synthesized TiO_2 and Degussa P25) were examined under visible light (Fig. 3a). Synthesized TiO_2 did not degrade 4–CP for the full reaction time of 4 h. Also, P25 demonstrated a poor ability to degrade 4-CP (24% degradation in 4 h), likely owing to the ligand-to-metal charge transfer (LMCT) pathway [23]. In contrast, Am-peroxo-TiO_2 can completely degrade 4-CP in 4 h. Measurements of chloride ion during the degradation of 4-CP indicates that approximately 66% of 4–CP degradation products were dechlorinated. Degradation of 4–CP with the xenon arc lamp system was 3.5-fold faster ($k_{4\text{-}CP}$ = 2.91 h^{-1}) than with the fluorescent lamp system ($k_{4\text{-}CP}$ = 0.83 h^{-1}) (Fig. S5 in the supplementary data), which can be reasonably explained by the difference in incident photon flows of the two systems (there was an approximately 3.8-fold difference, refer to Section 2.4 for the values). The TOC removal was approximately 20% during 41% degradation of 4–CP (0.1 mM 4–CP was initially used, data not shown).

Photochemical degradation of different organic compounds (phenol, 4–CP, BA, AAP, and CBZ) was examined in illuminated Am-peroxo-TiO_2 suspension (Fig. 3b). The degradation rate of AAP was the greatest (complete degradation in 1 h, k_{AAP} = 5.15 h^{-1}), which was followed by those of 4-CP and phenol ($k_{4\text{-}CP}$ = 0.83 h^{-1} and k_{Phenol} = 0.57 h^{-1}). However, BA and CBZ hardly degraded.

The effect of ·OH scavengers on the photochemical degradation of 4-CP was also examined (Fig. 3c); methanol and *tert*–butanol were used as the respective ·OH scavengers. It is believed that *tert*–butanol mainly scavenges free ·OH in the bulk phase, but methanol can scavenge both free and surface-bound ·OHs [24]. As shown in Fig. 3c, the addition of methanol and *tert*–butanol did not significantly affect the degradation rate of 4-CP by illuminated Am-peroxo-TiO_2. XTT (2,3-bis(2-methyl-4-nitro-5-sulfophenyl)-2H-tetrazolium-5-carboxanilide) was used as a probe for $O_2\cdot^-$. $O_2\cdot^-$ is known to reduce XTT to form XTT-formazan, which correspondingly displays a strong visible-light absorption band at 470 nm [25]. However, testing with XTT failed to detect any $O_2\cdot^-$ (Fig. S6 in the supplementary data). In addition, EPR analysis also failed to detect DMPO spin adducts of ·OH and $O_2\cdot^-$ (data not shown).

To examine the effects of dissolved oxygen, photochemical degradation 4-CP by illuminated Am-peroxo-TiO_2 was monitored under deaerated conditions (N_2 sparging), and compared with air-saturated conditions (open to the atmosphere) (Fig. 3d). Degradation of 4-CP was not significantly affected by deaeration, (only a marginal inhibition was observed), indicating that dissolved oxygen does not play an important role in the photochemical activity of Am-peroxo-TiO_2. This observation is inconsistent with an earlier study where TiO_2 photocatalysis in the presence of dissolved oxygen accelerated the degradation of organic compounds [26]. Specifically, oxygen captures electrons from the conduction band of TiO_2 (E_{CB} = −0.51 V_{NHE} at pH 7) to form $O_2\cdot^-$ ($E^0_{O_2/O_2\cdot^-}$ = −0.33 V) [27]. This electron trapping, in turn, is believed to inhibit the electron-hole recombination on the illuminated
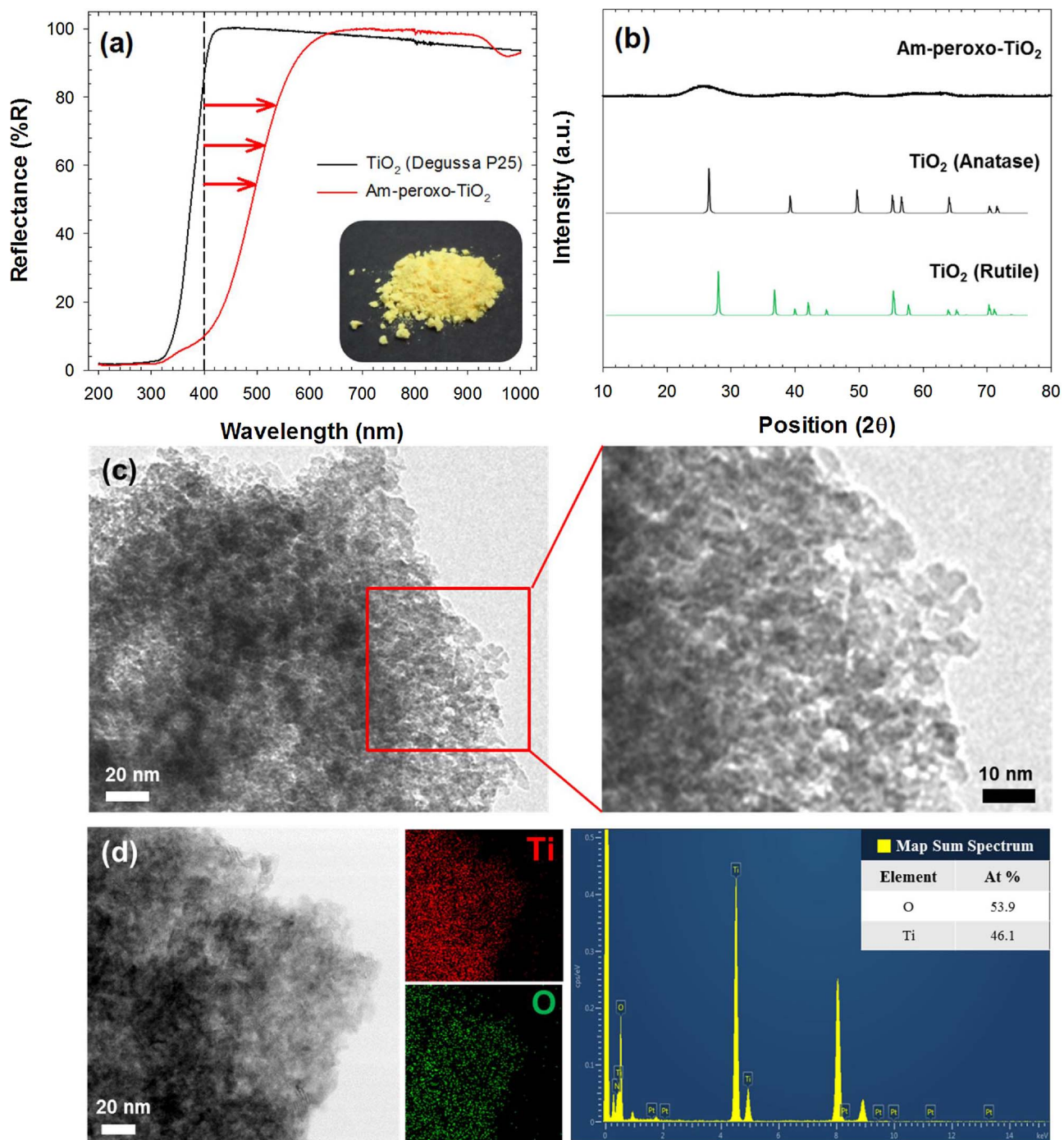
Fig. 1. (a) Diffuse reflectance spectra, (b) X-ray diffraction pattern, (c) HR-TEM image, and (d) EDX spectra of Am-peroxo-TiO₂.

TiO₂ surface, causing an increase in the steady-state concentration of oxidizing species in the valence band, which are ultimately responsible for degrading organic compounds.

3.3. Photostability of Am-peroxo-TiO₂

To evaluate the stability of Am-peroxo-TiO₂, repeated degradation of 4-CP in illuminated Am-peroxo-TiO₂ suspension was performed. Briefly, Am-peroxo-TiO₂ was added once at the beginning of the reaction, and 4–CP (1 µM) was injected every 2 h (Fig. 4a). The degradation efficiency of 4-CP decreased slightly over four cycles (open circles in Fig. 4a). Additionally, the Am-peroxo-TiO₂ suspension was pre-illuminated for 12 h in the absence of 4-CP, and then repeated degradation

with 4-CP was tested in the same manner (filled circles in Fig. 4a). The trends of 4-CP degradation of Am-peroxo-TiO₂ under pre-illuminated conditions almost synchronized with those of material that hadn't been pre-irradiated (compare open and filled circles in Fig. 4a), indicating that light illumination in the absence of an organic compound does not decrease the photochemical activity of Am-peroxo-TiO₂.

Repeated photocatalytic degradation was carried out with 4-CP, as previously described, with increasing concentrations of 4-CP (10 µM) as input (open circles in Fig. 4b). The degradation efficiency of 4-CP substantially decreased over the four cycles (99%, 65%, 35%, and 27% at each cycle). Note that the decrease in degradation efficiency with 1 µM 4-CP was minor (Fig. 4a). The decrease in 4-CP degradation efficiency is likely attributable to interference by accumulated oxidation
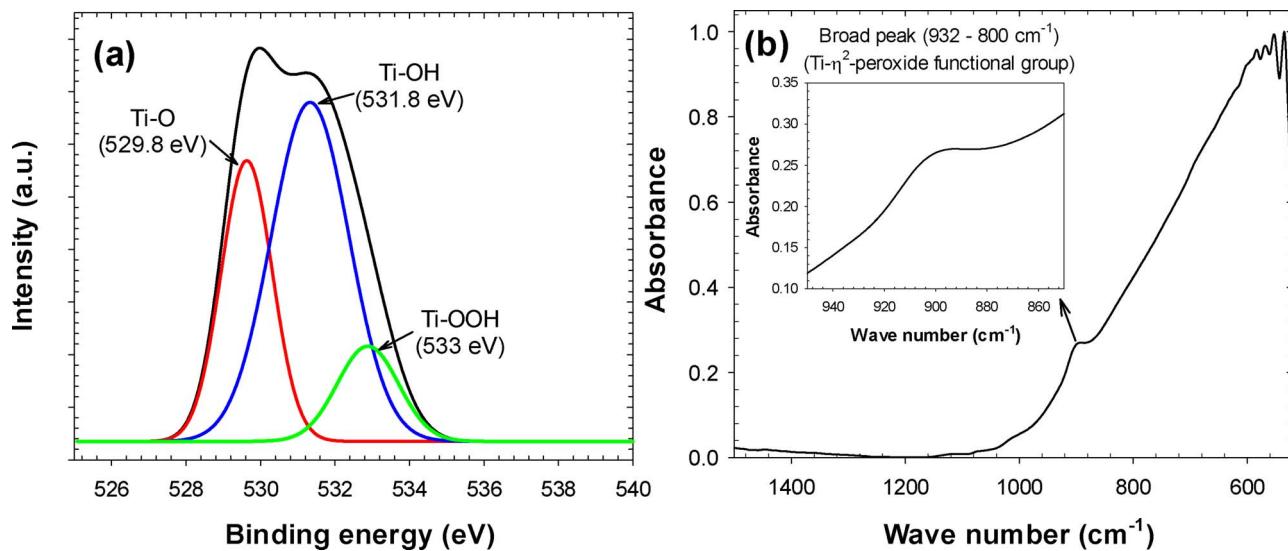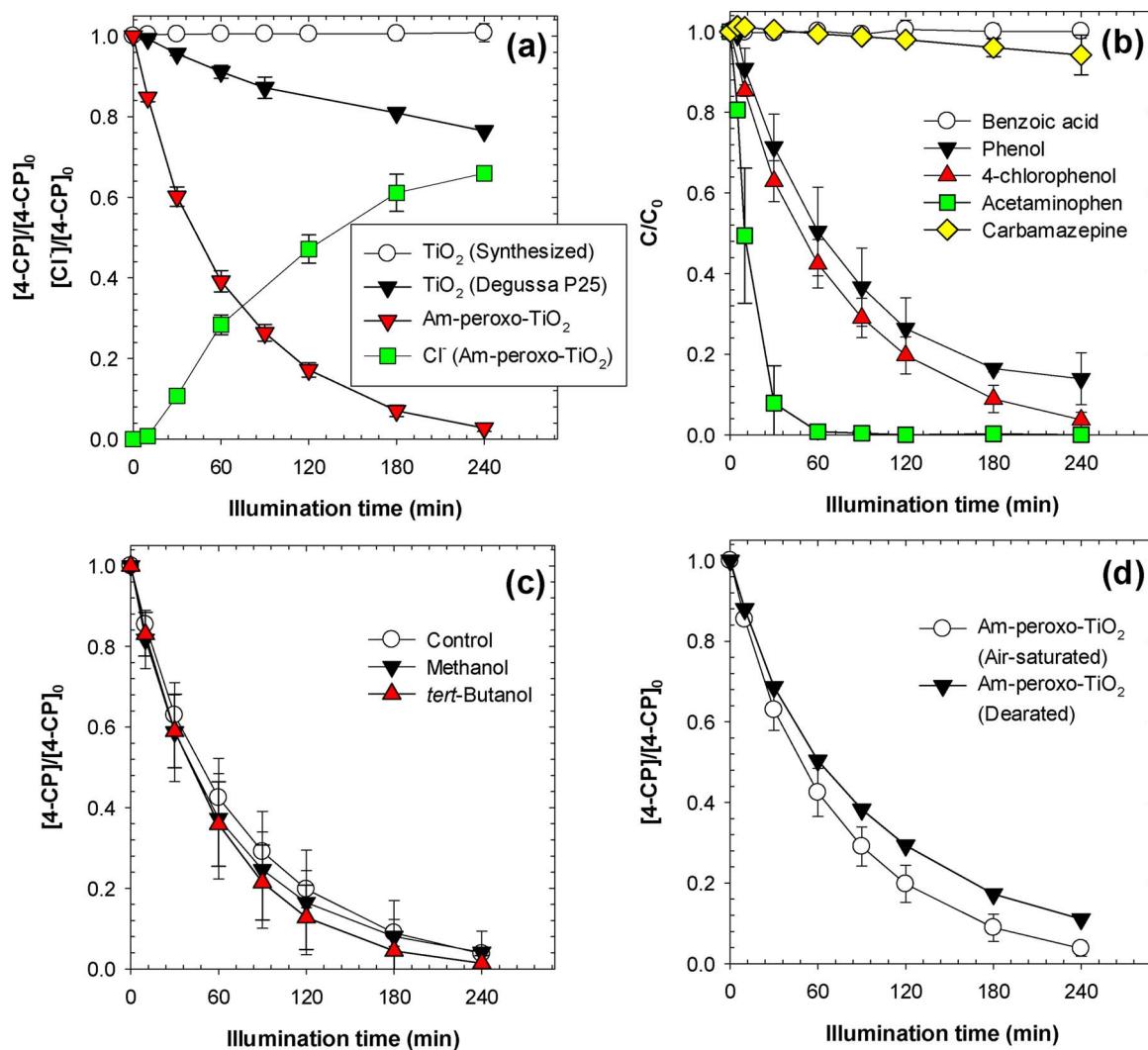
Fig. 2. (a) X-ray photoelectron spectra (O 1 s level) and (b) FT-IR spectra of Am-peroxo-TiO$_2$.

Fig. 3. Degradation of organic compounds by Am-peroxo-TiO$_2$ under visible-light illumination: (a) comparison with control TiO$_2$ photocatalysts and dechlorination of 4-CP by Am-peroxo-TiO$_2$ (b) degradation of different organic compounds, (c) effects of ROS scavengers, and (d) dissolved oxygen ([Am-peroxo-TiO$_2$] = 0.5 g/L, [4–CP]$_0$ = 10 μM, pH = 5, I = 6.43 × 10^{-6} Einstein/L s (fluorescent lamp, λ > 400 nm), [TiO$_2$]$_0$ = 0.5 g/L for (a), [BA]$_0$ = [Phenol]$_0$ = [AAP]$_0$ = [CBZ]$_0$ = 10 μM for (b); [Methanol]$_0$ = [*tert*-Butanol]$_0$ = 200 mM for (c)).

Fig. 4. Repeated degradation of 4-CP by Am-peroxo-TiO$_2$ (and Pt-Am-peroxo-TiO$_2$) under visible light illumination: (a) effect of pre-illumination and (b) comparison with Pt-Am-peroxo-TiO$_2$ ([Am-peroxo-TiO$_2$] = 0.5 g/L, pH = 5, I = 6.43 × 10^{-6} Einstein/L s (fluorescent lamp, λ > 400 nm), [4-CP]$_0$ = 1 μM for (a), [Pt-Am-peroxo-TiO$_2$]$_0$ = 0.5 g/L and [4–CP]$_0$ = 10 μM for (b)).
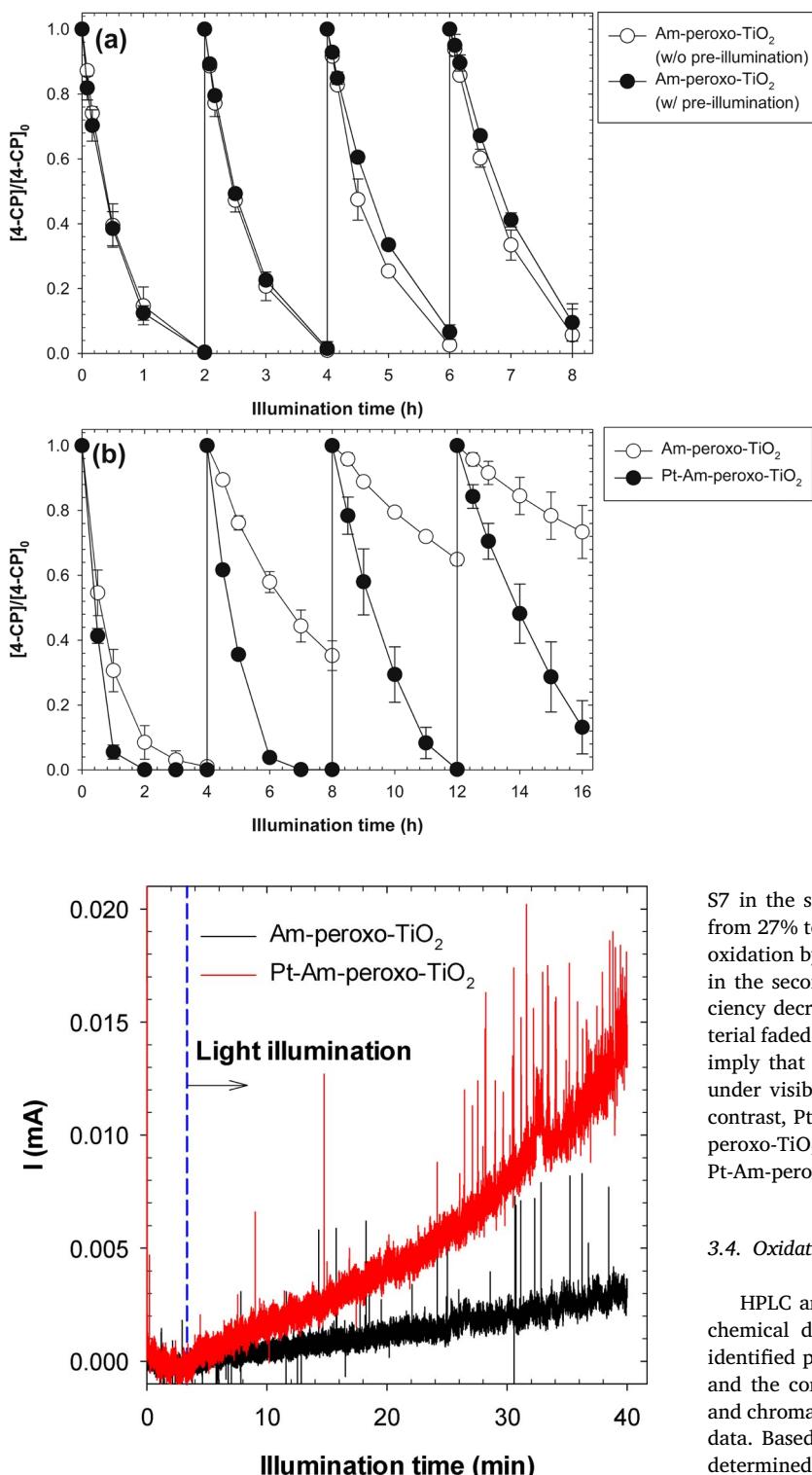
Fig. 5. Generation of Fe(III)/Fe(II) redox couple photocurrent of Am-peroxo-TiO$_2$ (and Pt-Am-peroxo-TiO$_2$) under visible light illumination ([Am-peroxo-TiO$_2$]$_0$ = [Pt-Am-peroxo-TiO$_2$]$_0$ = 0.5 g/L, [4–CP]$_0$ = 0.1 mM, [NaClO$_4$]$_0$ = 0.1 M, [Fe(III)]$_0$ = 1 mM, pH = 1.8, I = 2.46 × 10^{-5} Einstein/L s (xenon arc lamp, λ > 400 nm), working and counter electrodes = platinum plate (2.5 cm x 1.5 cm), reference electrode = calomel electrode, bias potential = +0.7 V).

products in the solution and on the material surface. To test this assumption, the used Am-peroxo-TiO$_2$ material was collected after four cycles of 4-CP degradation, rinsed with DI water three times, and resuspended in a new solution for another four-cycle repetition test (Fig.

S7 in the supplementary data). The degradation efficiency recovered from 27% to 65%, upon washing and resuspension, confirming that the oxidation byproducts partially contribute to the efficiency loss. Of note, in the second round of the repetition test, the 4-CP degradation efficiency decreased more rapidly. Strikingly, the yellow color of the material faded after the first repetition test. These observations collectively imply that surface peroxo-complexes of Am-peroxo-TiO$_2$ are unstable under visible light in the presence of specific organic compounds. In contrast, Pt-Am-peroxo-TiO$_2$ exhibited greater photostability than Am-peroxo-TiO$_2$ in the repetition test (filled circles in Fig. 4b); illuminated Pt-Am-peroxo-TiO$_2$ generated a higher photocurrent (Fig. 5).

3.4. Oxidation products of 4-CP

HPLC and LC/MS analyses identified 14 products from the photochemical degradation of 4-CP by illuminated Am-peroxo-TiO$_2$. The identified products were listed in Table S1 in the supplementary data, and the corresponding time-dependent variations of their abundance and chromatograms are presented in Figs. S8–S10 in the supplementary data. Based on these results, the degradation pathways of 4-CP were determined (Fig. 6).

4-Chlorocatechol (Product 7), hydroquinone (Product 2), and benzoquinone (Product 1) were the primary oxidation products of the reaction, which is consistent with previous observations of photocatalysis of 4-CP with bare TiO$_2$ [28–31]. Hydroquinone and benzoquinone were further oxidized to hydroxyquinol (Product 4), hydrobenzoquinone (Product 3), 1,2,4,5-benzenetetriol (Product 6), and 2,5-dihydroxy-1,4-benzoquinone (Product 5). 4-Chlorocatechol was further oxidized to chloromaleic acid (Product 8), (2E,4E)-3-chloro-2,4-hexadienedioic acid (Product 11), 5-chloro-1,2,4-benzenetriol (Product 10), and 4-chloro-5-hydroxy-1,2-benzoquinone (Product 9). In addition, bicyclic compounds such as dichlorobiphenyl (Product 14) and 5-chloro-2,4-dihydroxybiphenyl (Product 13) were also found.
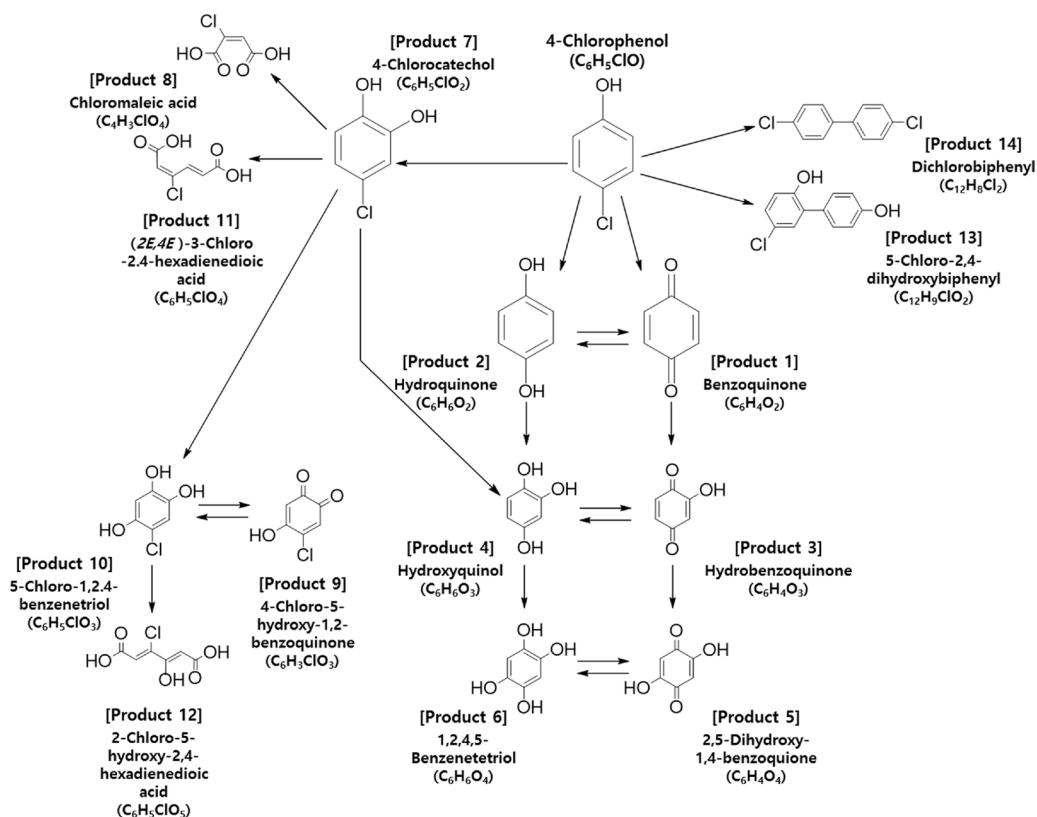
Fig. 6. Pathways depicting oxidative degradation of 4-CP by Am-peroxo-TiO$_2$ under visible light illumination.

4. Discussion

4.1. Photochemical activity of Am-peroxo-TiO$_2$

Am-peroxo-TiO$_2$ appears to demonstrate comparable or superior visible-light responsive photochemical activity to the photocatalysts reported in previous studies (although explicit comparison is difficult, given the nuances of experimental conditions such as the intensity and profile of incident light, etc.). In this study, photochemical degradation of 4-CP by Am-peroxo-TiO$_2$ was 96% in 4 h (Fig. 3a), which was more rapid than what was reported previously for nonmetal-doped TiO$_2$. For example, 4-CP degradation by N-doped TiO$_2$, S-doped TiO$_2$, and C/S-codoped TiO$_2$ was approximately 25%, 90%, and 35% in 3 h, 6 h, and 3 h, respectively, under visible light illumination using 150–300 W xenon arc and halogen lamps [32–34]. Ce/N-codoped TiO$_2$ and oxygen-rich TiO$_2$ exhibited faster degradation kinetics of organic dyes under visible-light illumination (100% and 98% degradation in 5 h and 3 h, respectively) [8,17]. Importantly, dyes used as target compounds can also serve as photosensitizers, thereby accelerating any photochemical processes. Additionally, Shankar et al. reported that peroxo-titania exhibited only a two-fold greater activity for methanol oxidation (to formaldehyde) than P25 under visible light illumination [15]. Note that the 4–CP degradation rate by Am-peroxo-TiO$_2$ was 9.6-fold greater than that of P25 (Fig. 3a)

4.2. Roles of ROS

Earlier studies on photochemical systems using TiO$_2$/H$_2$O$_2$ [13] and peroxo-titania [15] suggest that ·OH serves as a major reactive oxidant, and is responsible for the degradation of organic compounds. It has been suggested that photoexcited peroxo-titania complexes transfer electrons to the conduction band of TiO$_2$, facilitating the conversion of adsorbed H$_2$O$_2$ to ·OH by one-electron reduction.
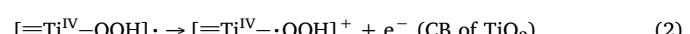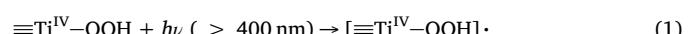
However, experimental results from this study present evidence against ·OH. The data suggests that Am-peroxo-TiO$_2$ may have different photochemical properties from other TiO$_2$ systems with peroxo-functionality that have been reported previously [13,15]. First, the selective degradation of organic compounds (Fig. 3b) cannot be explained by the reaction of ·OH since ·OH, a powerful oxidant ($E°$[·OH/H$_2$O] = +2.80 V$_{NHE}$), nonselectively oxidizes organic compounds at diffusion-controlled reaction rates ($>10^9$ M^{-1} s^{-1}) [35]. Second, the negligible effects of ·OH scavengers (methanol and *tert*-butanol) on 4-CP degradation also lends support to the idea that ·OH plays an insignificant role (Fig. 3c). In addition, when excess BA and coumarin were employed as ·OH probes in the illuminated Am-peroxo-TiO$_2$ suspension, the reaction did not yield the expected hydroxylated products (*p*-HBA and 7-HC), which implies that BA and coumarin were either not oxidized at all or were oxidized but do not produce hydroxylated products (Fig. S8).

Lastly, the XTT assay did not detect O$_2$·$^-$ in the illuminated Am-peroxo-TiO$_2$ suspension (Fig. S6), indicating that O$_2$·$^-$ does not affect 4-CP degradation.

4.3. Photochemical reactions of illuminated Am-peroxo-TiO$_2$

Photochemical reactions of illuminated Am-peroxo-TiO$_2$ are proposed in Fig. 7 (also refer to reactions 1 − 4 below). When surface Ti(IV)-peroxo complexes are photoexcited under visible-light illumination (reaction 1), an electron transfers to the conduction band (CB) of TiO$_2$, generating an oxidized peroxo intermediate ([≡Ti^{IV}−·OOH]$^+$) (reaction 2). Electron transfer from the CB to the surface peroxo complexes generates a reduced peroxo intermediate ([≡Ti^{III}−OOH]$^-$) (reaction 3). The two photogenerated intermediates ([≡Ti^{IV}−·OOH]$^+$ and [≡Ti^{III}−OOH]$^-$) immediately recombine on the surface (reaction 4). Am-peroxo-TiO$_2$ is stable under visible light illumination (Fig. 4a), as a result of rapid electron circulation that occurs through reactions 1 − 4.

$$\equiv Ti^{IV}-OOH + h\nu \ (\ > \ 400\,nm) \rightarrow [\equiv Ti^{IV}-OOH]· \tag{1}$$

$$[\equiv Ti^{IV}-OOH]· \rightarrow [\equiv Ti^{IV}-·OOH]^+ + e^- \ (CB \ of \ TiO_2) \tag{2}$$
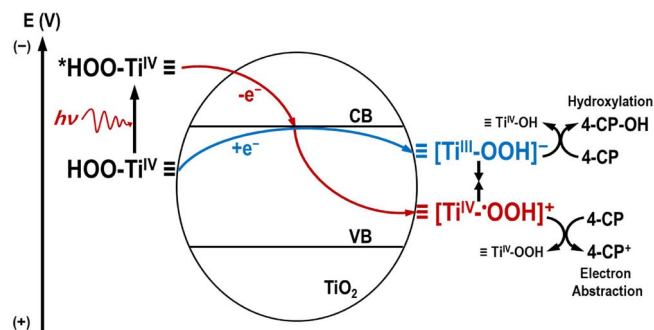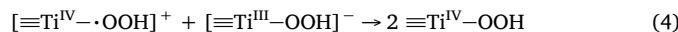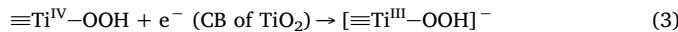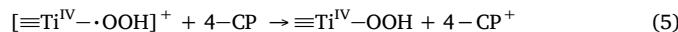
Fig. 7. Schematic diagrams of photochemical reactions occurring on visible light-illuminated Am-peroxo-TiO$_2$ (a) in the absence and (b) presence of organic compounds.

$$\equiv Ti^{IV}-OOH + e^- \ (CB \ of \ TiO_2) \rightarrow [\equiv Ti^{III}-OOH]^- \qquad (3)$$

$$[\equiv Ti^{IV}-\cdot OOH]^+ + [\equiv Ti^{III}-OOH]^- \rightarrow 2 \equiv Ti^{IV}-OOH \qquad (4)$$
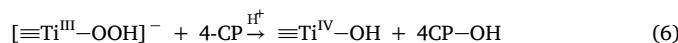
4.4. Mechanism of organic compound degradation by illuminated Am-peroxo-TiO$_2$

The data suggests that the two photogenerated intermediates ($[\equiv Ti^{IV}-\cdot OOH]^+$ and $[\equiv Ti^{III}-OOH]^-$) are responsible for the oxidative degradation of organic compounds (Fig. 7). These intermediates, $[\equiv Ti^{IV}-\cdot OOH]^+$ and $[\equiv Ti^{III}-OOH]^-$, are believed to exhibit similar properties to surface-bound HO$_2\cdot$ and $\cdot$OH, respectively. $[\equiv Ti^{IV}-\cdot OOH]^+$ can oxidize specific organic compounds (e.g., 4-CP) via an electron abstraction mechanism (reaction 5).

$$[\equiv Ti^{IV}-\cdot OOH]^+ + 4-CP \rightarrow \equiv Ti^{IV}-OOH + 4-CP^+ \qquad (5)$$

$[\equiv Ti^{III}-OOH]-$, which possesses $\cdot$OH-like properties (e.g., $[\equiv Ti^{III}-OOH]^- \leftrightarrow [\equiv Ti^{IV}-O-\ldots\cdot OH]$), is assumed to hydroxylate a given organic compound (reaction 6).

$$[\equiv Ti^{III}-OOH]^- + 4-CP \xrightarrow{H^+} \equiv Ti^{IV}-OH + 4CP-OH \qquad (6)$$

The primary products of 4-CP oxidation (4-chlorocatechol (Product 7), hydroquinone (Product 2), and benzoquinone (Product 1)) can form via reactions initiated by electron abstraction and hydroxylation of 4-CP, as described in Fig. 8.

The loss of activity arising from illuminated Am-peroxo-TiO$_2$ in the repetition test with 4-CP degradation (Fig. 4) can be attributed to the destruction of surface peroxo groups by the reaction of $[\equiv Ti^{III}-OOH]^-$ with 4-CP (reaction 6). XPS data revealed that surface peroxo groups on Am-peroxo-TiO$_2$ almost disappeared after the reaction (Figs. S11a and S11b in the supplementary data). Diffuse reflectance also increased after the reaction (Fig. S12a in the supplementary data), which coincided with the fading of the yellow color of the powdered material.

Pt-Am-peroxo-TiO$_2$ exhibited enhanced photostability in the presence of 4-CP (Fig. 4b). Namely, the loss of surface peroxo groups was relatively small (Figs. S11c and S11d in the supplementary data), and the increase in diffuse reflectance was also minor (Fig. S12b in the supplementary data). It is believed that the Pt deposits trap electrons from the CB of TiO$_2$ [36] (also evidenced by the enhanced generation of photocurrents (Fig. 5)), thereby inhibiting the formation of $[\equiv Ti^{III}-OOH]^-$ and reducing the subsequent loss of peroxo groups (reaction 6). The suppressed formation of $[\equiv Ti^{III}-OOH]^-$ also inhibited the recombination of $[\equiv Ti^{IV}-\cdot OOH]^+$ and $[\equiv Ti^{III}-OOH]^-$ (reaction 4), which caused an enhancement of photochemical activity of the material; 4-CP degradation by Pt-Am-peroxo-TiO$_2$ occurs more rapidly than with Am-peroxo-TiO$_2$ (Fig. 4b). Although it has been reported that the redox states of Pt defects in the TiO$_2$ lattice can improve visible-light absorption [37], such an effect was not seen with our materials when comparing the reflectance spectra of Am-peroxo-TiO$_2$ and Pt-Am-peroxo-TiO$_2$ (Figs. S12a and S12b).

4-CP degradation via the LMCT mechanism of $\equiv TiO_2-4$-CP complexes was also ruled out. The minor effects of oxygen in this system (Fig. 3d) contrasts those observed with the LMCT mechanism, in which oxygen acts as an electron acceptor to significantly accelerate 4-CP degradation by trapping electrons from surface complexes [23]. In this study, oxygen had a minor effect. Furthermore, in our proposed mechanism the negligible effect of oxygen suggests that oxygen fails to capture electrons from the CB of TiO$_2$ (possibly due to the rapid transit of CB electrons to the surface peroxo complexes), and correspondingly fails to abstract electrons from $[\equiv Ti^{III}-OOH]^-$. In addition, the positive effect of platiniazation (Fig. 4b) contradicts the LMCT mechanism, as Pt deposition acts as physical barriers, which is known to inhibit the formation of charge-transfer complexes of TiO$_2$ with the organic compound [23,38].

5. Conclusions

In this study, a novel visible light responsive photosensitizer

Fig. 8. Proposed mechanisms for primary oxidation of 4-CP by visible light-illuminated Am-peroxo-TiO$_2$.
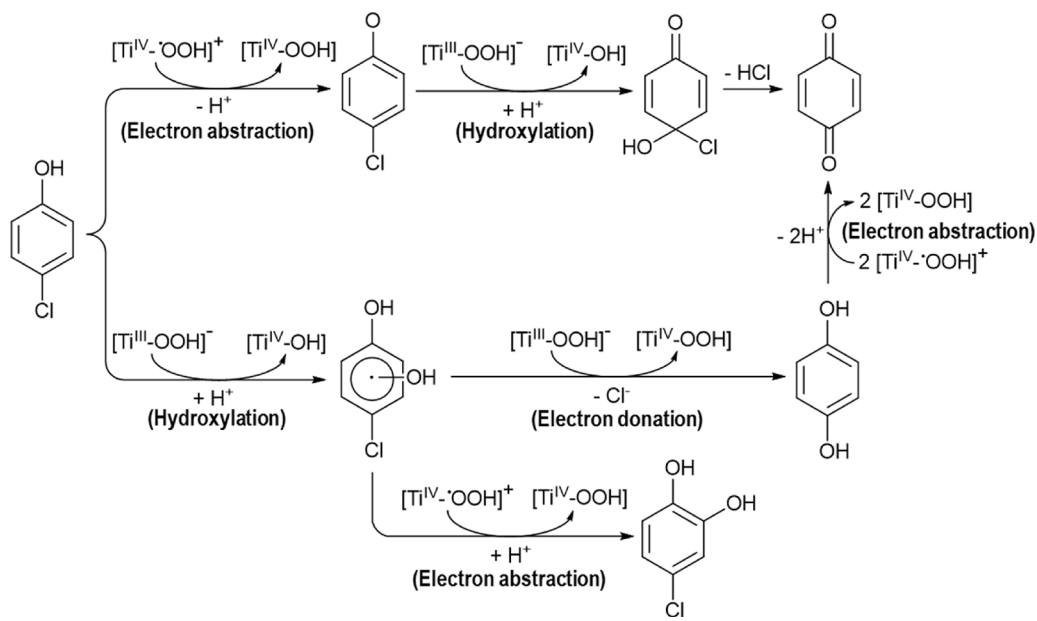
(Am−peroxo−TiO$_2$) was synthesized by a facile method using titanium isopropoxide and H$_2$O$_2$ under mild conditions. Am-peroxo-TiO$_2$ was found to form aggregates of small amorphous titania nanoparticles with surface peroxo complexes. Am-peroxo-TiO$_2$ exhibited excellent but selective photochemical activity in degrading select organic compounds. Importantly, the roles of ROS such as ·OH and O$_2$·$^-$ were found to be insignificant. Photogenerated reactive intermediates on the surface (i.e., [≡Ti^{IV}−·OOH]$^+$ and [≡Ti^{III}−OOH]$^-$) may be responsible for the degradation of select organic compounds. These reactive species are assumed to oxidize 4-CP via a series of electron abstraction and hydroxylation reactions. In the absence of any organic compounds, Am-peroxo-TiO$_2$ was stable under both dark and illuminated conditions. However, both light illumination and the presence of organic compounds gradually destroyed the surface peroxo complexes of Am-peroxo-TiO$_2$, causing a decrease in its photochemical activity. To counter this, Pt-loading was found to be an effective method to enhance the photostability and photochemical activity of Am-peroxo-TiO$_2$.

Acknowledgments

Appendix A. Supplementary data

Supplementary data associated with this article can be found, in the online version, at https://doi.org/10.1016/j.apcatb.2017.12.009.

References

[1] M.R. Hoffmann, S.T. Martin, W. Choi, D.W. Bahnemann, Chem. Rev. 95 (1995) 69–96.
[2] U.I. Gaya, A.H. Abdullah, J. Photochem. Photobiol. C-Photochem. Rev. 9 (2008) 1–12.
[3] A.R. Khataee, M.B. Kasiri, J. Mol. Catal. A-Chem. 328 (2010) 8–26.
[4] M. Pelaez, N.T. Nolan, S.C. Pillai, M.K. Seery, P. Falaras, A.G. Kontos, P.S.M. Dunlop, J.W.J. Hamilton, J.A. Byrne, K. O'Shea, M.H. Entezari, D.D. Dionysiou, Appl. Catal. B-Environ. 125 (2012) 331–349.
[5] R. Vinu, G. Madras, Environ. Sci. Technol. 42 (2008) 913–919.
[6] H. Einaga, M. Harada, S. Futamura, T. Ibusuki, J. Phys. Chem. B 107 (2003) 9290–9297.
[7] W. Kim, T. Tachikawa, H. Kim, N. Lakshminarasimhan, P. Murugan, H. Park, T. Majima, W. Choi, Appl. Catal. B-Environ. 147 (2014) 642–650.
[8] M. Nasir, S. Bagwasi, Y. Jiao, F. Chen, B. Tian, J. Zhang, J. Chem Eng 236 (2014) 388–397.
[9] M.C. Yin, Z.S. Li, J.H. Kou, Z.G. Zou, Environ. Sci. Technol. 43 (2009) 8361–8366.
[10] H. Kyung, J. Lee, W. Choi, Environ. Sci. Technol. 39 (2005) 2376–2382.
[11] D. Zhao, C.C. Chen, C.L. Yu, W.H. Ma, J.C. Zhao, J. Phys. Chem. C 113 (2009) 13160–13165.
[12] Y. Bessekhouad, D. Robert, J. Weber, J. Photochem. Photobiol. A-Chem. 163 (2004) 569–580.
[13] X. Li, C. Chen, J. Zhao, Langmuir 17 (2001) 4118–4122.
[14] T. Ohno, Y. Masaki, S. Hirayama, M. Matsumura, J. Catal. 204 (2001) 163–168.
[15] M.V. Shankar, T. Kako, D.W.J. Ye, J. Colloid Interf. Sci. 331 (2009) 132–137.
[16] T. Liu, X. Li, X. Yuan, Y. Wang, F. Li, J. Mol. Catal. A-Chem. 414 (2016) 122–129.
[17] V. Etacheri, M.K. Seery, S.J. Hinder, S.C. Pillai, Adv. Funct. Mater. 21 (2011) 3744–3752.
[18] L.-L. Tan, W.-J. Ong, S.-P. Chai, A.R. Mohamed, Chem. Commun. 50 (2014) 6923–6926.
[19] E.E. Wegner, A.W. Adamson, J. Am. Chem. Soc. 80 (1966) 394–404.
[20] Y. Park, S.H. Kang, W. Choi, Phys. Chem. Chem. Phys 13 (2011) 9425–9431.
[21] Y. Gao, Y. Masuda, K. Koumoto, Langmuir 20 (2004) 3188–3194.
[22] G. Munuera, A.R. González-Elipe, A. Fernández, P. Malet, J.P. Espinós, J. Chem. Soc. Faraday Trans. 1 (85) (1989) 1279–1290.
[23] S. Kim, W. Choi, J. Phys. Chem. B 109 (2005) 5143–5149.
[24] M. Cho, H. Chung, W. Choi, J. Yoon, Appl. Environ. Microbiol. 71 (2005) 270–275.
[25] L. Brunet, D.Y. Lyon, E.M. Hotze, P.J.J. Alvarez, M.R. Wiesner, Environ. Sci. Technol. 43 (2009) 4355–4360.
[26] S. Kim, W. Choi, J. Phys. Chem. B 106 (2002) 13311–13317.
[27] H. Park, Y. Park, W. Kim, W. Choi, J. Photochem. Phobiol. C-Photochem. Rev. 15 (2013) 1–20.
[28] J. Theurich, M. Lindner, D.W. Bahnemann, Langmuir 12 (1996) 6368–6376.
[29] K. Vinodgopal, U. Stafford, K.A. Gray, P.V. Kamat, J. Phys. Chem. 98 (1994) 6796–6803.
[30] X. Li, J.W. Cubbage, T.A. Tetzlaff, W.S. Jenks, J. Org. Chem. 64 (1999) 8509–8524.
[31] X. Li, J.W. Cubbage, W.S. Jenks, J. Org. Chem. 64 (1999) 8525–8536.
[32] S. Sakthivel, M. Janczarek, H. Kisch, J. Phys. Chem. B 108 (2004) 19384–19387.
[33] W. Ho, J.C. Yu, S. Lee, J. Solid State Chem. 179 (2006) 1171–1176.
[34] H. Sun, Y. Bai, Y. Cheng, W. Jin, N. Xu, Ind. Eng. Chem. Res. 45 (2006) 4971–4976.
[35] G.V. Buxton, C.L. Greenstock, W.P. Helman, A.B. Ross, J. Phys. Chem. Ref. Data 17 (1988) 513–886.
[36] J. Kim, J. Lee, W. Choi, Chem. Commun. 6 (2008) 756–758.
[37] S. Kim, S.-J. Hwang, W. Choi, J. Phys. Chem. B 109 (2005) 24260–24267.
[38] G. Kim, W. Choi, Appl. Catal. B-Environ. 100 (2010) 77–83.